J Periodontal Implant Sci. 2023 Jun;53(3):218-232
https://doi.org/10.5051/jpis.2300660033
pISSN 2093-2278·eISSN 2093-2286

JPIS
Journal of Periodontal & Implant Science

Research Article
Implant Science

Check for updates

Sinus augmentation with poly(ε) caprolactone-β tricalcium phosphate scaffolds, mesenchymal stem cells and platelet rich plasma for one-stage dental implantation in minipigs

Jeong-Hun Nam [1,†], **Akram Abdo Almansoori** [1,2,†], **Oh-Jun Kwon** [1], **Young-Kwon Seo** [3], **Bongju Kim** [2], **Young-Kyun Kim** [4], **Jong-Ho Lee** [2,5], **KangMi Pang** [6,*]

[1]Department of Oral & Maxillofacial Surgery, School of Dentistry, Seoul National University, Seoul, Korea
[2]Dental Life Science Research Institute, Innovation Research & Support Center for Dental Science, Seoul National University Dental Hospital, Seoul, Korea
[3]Department of Chemical and Biochemical Engineering, College of Engineering, Dongkuk University, Seoul, Korea
[4]Department of Oral & Maxillofacial Surgery, Section of Dentistry, Seoul National University Bundang Hospital, Seongnam, Korea
[5]Oral Oncology Clinic, National Cancer Center, Ilsan, Korea
[6]Department of Oral & Maxillofacial Surgery, Seoul National University Gwanak Dental Hospital, Seoul, Korea

Received: Jan 13, 2023
Revised: Mar 10, 2023
Accepted: Apr 3, 2023
Published online: May 12, 2023

***Correspondence:**
KangMi Pang
Department of Oral and Maxillofacial Surgery, Seoul National University Gwanak Dental Hospital, 1 Gwanak-ro, Gwanak-gu, Seoul 08826, Korea.
Email: pkm81@snu.ac.kr
Tel: +82-2-6747-6114
Fax: +82-2-6747-6519

[†]Jeong-Hun Nam and Akram Abdo Almansoori contributed equally as first authors.

ORCID iDs
Jeong-Hun Nam
https://orcid.org/0000-0003-3957-0476
Akram Abdo Almansoori
https://orcid.org/0000-0001-7134-9195
Oh-Jun Kwon
https://orcid.org/0000-0002-0457-6539
Young-Kwon Seo
https://orcid.org/0000-0001-7533-9605
Bongju Kim
https://orcid.org/0000-0001-7309-5977
Young-Kyun Kim
https://orcid.org/0000-0002-7268-3870
Jong-Ho Lee
https://orcid.org/0000-0002-8843-545X
KangMi Pang
https://orcid.org/0000-0001-9148-9080

ABSTRACT

Purpose: This study evaluated the efficacy of a tube-shaped poly(ε) caprolactone - β tricalcium phosphate (PCL-TCP) scaffold with the incorporation of human umbilical cord-derived mesenchymal stem cells (hUCMSCs) and platelet-rich plasma (PRP) for bone regeneration in the procedure of single-stage sinus augmentation and dental implantation in minipigs.
Methods: Implants were placed in the bilateral sides of the maxillary sinuses of 5 minipigs and allocated to a PCL-TCP+hUCMSCs+PRP group (n=5), a PCL-TCP+PRP group (n=5), and a PCL-TCP-only group (n=6). After 12 weeks, bone regeneration was evaluated with soft X-rays, micro-computed tomography, fluorescence microscopy, and histomorphometric analysis.
Results: Four implants failed (2 each in the PCL-TCP+hUCMSCs+PRP and PCL-TCP+hUCMSC groups). An analysis of the grayscale levels and bone-implant contact ratio showed significantly higher mean values in the PCL-TCP+hUCMSCs+PRP than in the PCL-TCP group (P=0.045 and P=0.016, respectively). In fluoromicroscopic images, new bone formation around the outer surfaces of the scaffolds was observed in the PCL-TCP+hUCMSCs+PRP group, suggesting a tenting effect of the specially designed scaffolds. Bone regeneration at the scaffold-implant interfaces was observed in all 3 groups.
Conclusions: Using a tube-shaped, honeycombed PCL-TCP scaffold with hUCMSCs and PRP may serve to enhance bone formation and dental implants' osseointegration in the procedure of simultaneous sinus lifting and dental implantation.

Keywords: Dental implants; Platelet-rich plasma; Sinus floor augmentation; Stem cells

Funding

This research was supported by a grant from the Korea Health Technology R&D Project through the Korea Health Industry Development Institute and funded by the Ministry of Health and Welfare, Republic of Korea (HI20C2114).

Conflict of Interest

No potential conflict of interest relevant to this article was reported.

Author Contributions

Conceptualization: Jong-Ho Lee; Data curation: Oh-Jun Kwon, Jeong-Hun Nam; Formal analysis: Kilhyun Nam; Investigation: Oh-Jun Kwon, Jeong-Hun Nam; Methodology: Jong-Ho Lee, Young-Kwon Seo, Bongju Kim; Software: Akram Abdo Almansoori; Supervision: Jong-Ho Lee, KangMi Pang; Validation: Akram Abdo Almansoori, Young-Kyun Kim, Jong-Ho Lee; Writing - original draft: Jeong-Hun Nam; Writing - review & editing: Akram Abdo Almansoori, Jong-Ho Lee, KangMi Pang.

INTRODUCTION

Maxillary sinus lifting has become an important procedure for patients with poor bone height and severe sinus pneumatization [1]. In such situations, particulate autogenous bone grafting has been frequently used. However, this procedure has difficulties in the approximation of affixing graft materials to the implant, weak holding effects, the possibility of material leakage through the mucosal perforation, poor packing effects, and potential donor site morbidities [2,3]. Particulate allograft, xenograft, and synthetic graft materials have similar problems. Due to these problems, 2-stage dental implantation techniques are generally recommended in the procedure of sinus grafting with particulate bone substitutes when initial stability of the implant has not been achieved [4].

To overcome the limitations of particulate bone graft materials, a conformational change to the graft materials was considered. Poly-(ε-caprolactone) (PCL), an aliphatic polyester, is known as an effective bone-scaffolding application due to its slow degradation, and the use of PCL in medical devices has been approved by the US Food and Drug Administration [5]. However, PCL scaffolds have limitations, such as long degradation times, hydrophobicity, and poor osteoconduction, osteoinduction, and osteointegration [6]. Combining PCL with β-tricalcium phosphate (TCP) showed increased mechanical properties and cellular proliferation when used as the 3-dimensional (3D) printed bone graft material or membrane for guided bone regeneration [6-8]. In this study, we fabricated 3D, tube-shaped, biodegradable scaffolds using a PCL/TCP composite through rapid prototyping technology [9]. This design was expected to increase the primary stability of the implant despite insufficient bone height of the maxillary sinus floor by holding the sinus part of the implant with a screw-like mechanism. Incorporating TCP has been reported to encourage osteoblast differentiation and mineralization among human bone marrow cells both *in vitro* and *in vivo* [10], and to ease cell loading and decrease stem cell loss in porous scaffold structures [11]. It is known that mesenchymal stem cells (MSCs) provide an osteogenic cell source for new bone formation, and that platelet-rich plasma (PRP) supports the expansion, differentiation and *in vivo* bone formation capacity of MSCs [12,13]. Transplantation of MSCs and PRP on a hydroxyapatite scaffold significantly enhanced bone formation in sinus lift procedures compared to using the scaffold alone [12].

Therefore, this study evaluated the efficacy of a tube-shaped, honeycombed PCL-TCP scaffold with the incorporation of human umbilical cord-derived mesenchymal stem cells (hUCMSCs) and PRP for bone regeneration in the procedure of single-stage sinus lifting and dental implantation in minipigs.

MATERIALS AND METHODS

Fabrication of tube-shaped PCL-TCP scaffolds

PCL-TCP (80%:20%) composite scaffolds (Osteopore International Pte. Ltd., Singapore) were fabricated using fused deposition modeling methods as described in previous reports [14,15]. Each scaffold had a lay-down pattern of 0°, 60°, and 120° cross-linking, a porosity of 70%, and an average pore size of 0.515 mm, as determined by micro-computed tomography (CT) analysis. The tube-shaped structures of the PCL-TCP scaffolds were made of 3D interwoven bioresorbable polymer filaments in a honeycomb array of interconnected equilateral triangles with a regular porous morphology [16,17]. The scaffolds were specially

https://doi.org/10.5051/jpis.2300660033

JPIS
Journal of Periodontal & Implant Science

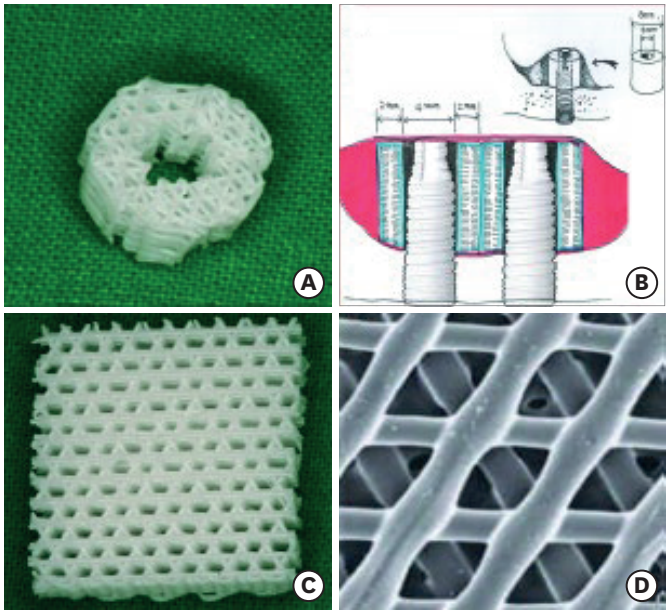

Figure 1. Structures of the specially designed, tube-shaped PCL-TCP scaffold. (A) Each tube-shaped PCL-TCP scaffold with male-female screw designs had an outer diameter of 8.0 mm, inner diameter of 4.0 mm, and height of 4.0 mm. The inner diameter of the PCL-TCP scaffold was designed to fit within the diameter of the implant fixture in this study. (B) Schematic drawing of dental implantation and simultaneous maxillary sinus lifting with the PCL-TCP scaffold. (C) and D) Magnified views of the scaffold with the interconnected honeycomb structures at about 70% porosity.
PCL-TCP: poly-(ε-caprolactone)/β-tricalcium phosphate.

designed and manufactured such that their inner diameter would fit the outer diameter of the implant fixture. They had an inner diameter of 4.0 mm, an outer diameter of 8.0 mm, a height of 4.0 mm, and a thickness of 2.0 mm (**Figure 1**). The scaffolds were sterilized using low-temperature (36.5°C) ethylene oxide gas suitable for animal surgery.

Preparation of hUCMSCs

The hUCMSCs were obtained from the Research Institute of Biotechnology at Dongguk University, Korea. After the hUCMSCs were isolated and cultured, their characterization was analyzed using a fluorescence-activated cell-sorter. It was determined that the cells were positive for CD73, CD90, CD105, and CD166 markers and negative for CD14, CD31, CD34, and CD45 markers. In addition, the cells were induced to differentiate into osteocytes, chondrocytes, and adipocytes [18]. According to these results, the isolated and cultured cells could be identified as hUCMSCs.

Next, the cells were cultured for expansion. After 5 passages, the hUCMSCs were prepared for transplantation into each of the PCL-TCP scaffolds.

Preparation of PRP

Whole blood samples (200 mL) were collected from each minipig's internal jugular vein just before the experimental surgery. The blood was prepared with anticoagulation agents (EDTA 0.2 g/50 mL blood), and it was centrifuged for 5 minutes at 3,200 rpm. Buffy-coat plasma was acquired and was centrifuged again for 5 minutes at 5,200 rpm. Next, the PRP in the lower middle portion of the second centrifuged plasma sample was collected, resulting in a 1.0–1.5 mL/50 mL concentration of PRP. For the activation of PRP, thrombin (1,000 units, Dirabine® powder; Korea United Pharm. Inc., Seoul, Korea) and calcium gluconate ($CaCl_2$, 100 mg/mL,

https://doi.org/10.5051/jpis.2300660033

JPIS Journal of Periodontal & Implant Science

Calmia® Inj.; Korea United Pharm. Inc.) were mixed in the same proportion (1:1), and this solution was then mixed with the PRP at a 1:6 volume ratio to act as the gel phase.

Animal grouping and surgery

This research was approved by the Standing Ethical Committee for Animal Research of the Laboratory in the Clinical Research Institute of Medi Kinetics (Medi Kinetics-IACUC: 100125001). Five male minipigs (Medi Kinetics Micropigs; Medi Kinetics Co., Pyeongtaek, Korea), aged 12.5 to 17.5 months (32.8 to 41.0 kg), were used. In total, after sinus lifting, 20 dental implantations were performed, 2 each per maxillary sinus in 5 minipigs. The 3 experimental groups consisted of a dental implantation and simultaneous maxillary sinus lifting with hUCMSCs and PRP loaded into the PCL-TCP scaffold (PCL-TCP+hUCMSCs+PRP) group, PRP loaded into the PCL-TCP scaffold (PCL-TCP+PRP) group, and a similar group with only the PCL-TCP scaffold (PCL-TCP) (**Table 1**).

All surgical procedures were performed under general anesthesia. Sinus lifting was performed with an infraorbital access after an inverted L incision on the infraorbital area [19]. Direct access to the sinus was achieved below the malar prominence using a surgical bur. After elevation of the Schneiderian membrane, 2 submerged dental implants (Osstem GSII®; Osstem Implant Co., Seoul, Korea) measuring 10.0 mm in length and 4.0 mm in width were placed at each zygomatico-maxillary buttress area. During the dental implantation procedures, the stem cells were seeded onto the scaffold (4.0×10^7 cells/scaffold) using a micropipette by a drop-down and soak method. Then, the PRP was loaded onto each scaffold (0.2–0.5 mL/scaffold). After dental implantation with sinus lifting, the inner hole of each scaffold was fitted to the outer surface of its implant fixture, which was extruded into the elevated sinus cavities (**Figure 2**). The wounds were cared for with skin dressings and

Table 1. Densitometric analysis using soft X-rays

Group	No.	Gray level	New bone area%
PCL-TCP+hUCMSCs+PRP	5	102.48±68.38[a)]	23.3±7.9
PCL-TCP+PRP	5	88.09±66.62	22.9±5.9
PCL-TCP	6	58.10±29.69[a)]	20.1±5.9

Values are presented as mean ± standard deviation.
PCL-TCP: poly-(ε-caprolactone)/β-tricalcium phosphate, hUCMSC: human umbilical cord-derived mesenchymal stem cell, PRP: platelet-rich plasma.
[a)]A statistically significant difference between the PCL-TCP+hUCMSCs+PRP group and the PCL-TCP group was found, $P<0.05$, using analysis of variance with the *post hoc* Fisher protected least significant difference test.

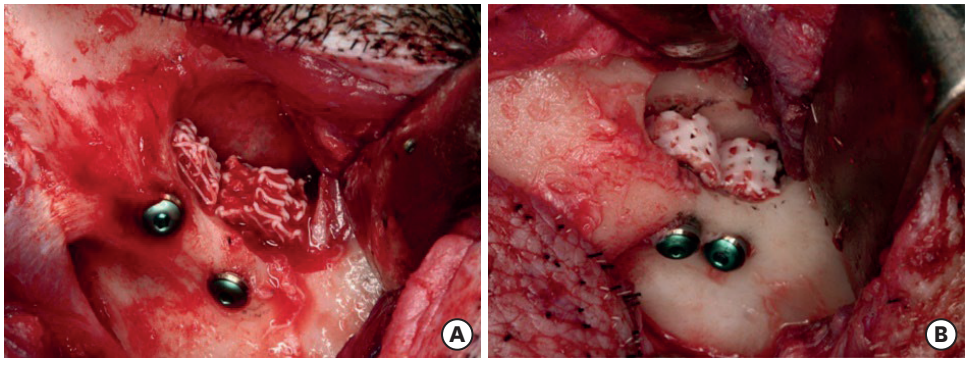

Figure 2. Intraoperative photographs showing dental implantation and simultaneous sinus lifting with delivery of human umbilical cord-derived mesenchymal stem cells and platelet-rich plasma into the PCL-TCP scaffold (A) and with only the PCL-TCP scaffold (B).
PCL-TCP: poly-(ε-caprolactone)/β-tricalcium phosphate.

https://doi.org/10.5051/jpis.2300660033

JPIS Journal of Periodontal & Implant Science

medication for 1 to 3 days using oxytetracycline (3 mL, intramuscular [IM]) (Green Cross Corp., Yongin, Korea) and flunixin meglumine (2 mL, IM) (Green Cross Corp.).

Fluorescence labeling

To evaluate the histological chronology of regenerative bone formation, 3 fluorochromes were administered to each of the 5 minipigs in the predefined sequence used for polychromic bone labeling. Calcein was dissolved in 0.9% NaCl with a 10 mg/kg density, and then 2% sodium bicarbonate was added to bring the pH to 7.2. Alizarin red and tetracycline HCl were dissolved in distilled water. All reagents (Sigma-Aldrich Co. Ltd., St. Louis, MO, USA) were injected intramuscularly through a 0.2 μm syringe-filtering sterilization. Tetracycline HCl (600 mg; 15 mg/kg) was administered at 3 and 11 weeks postoperatively, calcein (400 mg; 10 mg/kg) was administered at 6 weeks, and alizarin red (1200 mg; 30 mg/kg) was administered at 9 weeks.

Harvesting of the specimen

Twelve weeks postoperatively, the minipigs were sacrificed and their jaw bones were harvested. Internal fixation with 4% paraformaldehyde (PFA) and external fixation with 10% PFA at 4°C was performed.

Evaluation

CT Scan

Paranasal sinus CT (Somaton Sensation 10, Siemens, Germany; 1.5 mm slice thickness and 1.0 mm table speed) was used to perform clinical evaluations of the postoperative implant-scaffold stability, new bone formation, and postoperative complications.

Soft radiogram scan and densitometric analysis

From the axial CT scan information, cube-shaped blocks 2.0 cm long on each side, including the dental implants and PCL-TCP scaffolds, were harvested by cutting the specimen parallel to the implant's long axis. Radiograms were taken using a cabinet-style soft X-ray unit (CMB-2, Softex Co. Japan; 30 KVp, 2 mA, and exposure time of 90 seconds). Radiodensity was analyzed using 5 randomly chosen points in the regenerated area and the normal host bone area (OPTIMAS, version 6.51.199; Media Cybernetics, L.P., Rockville, MD, USA). Then, using captured images, the average grayscale level and the percentage of the area that had regenerated were evaluated as the percentage ratio of the new bone area to that of the experimental area.

Micro-CT scan and 3D bone morphogenic analysis

X-ray microtomography systems (Skyscan 1072/1172, ver. 1.5, Belgium) were used to obtain micro-CT images under the conditions of magnification (×14), source 80 kV/100 mA, rotation 180°, rotation step 0.90°, exposure time 3.4 sec and no filtering. These original data images (TIFF files) were converted to digital bitmap images (BMP format) using NRecon® software (ver. 1.5.1.3, Skyscan; Bruker, Kontich, Belgium). To assure optimal digital images with minimal beam-hardening effects (0.7000 Hounsfield units [HU] to 0.1000 HU in the 1072 system and 0.1100 HU to 0.0030 HU in the 1172 system), a reference HU value was used. The digital bitmaps were analyzed using non-invasive 3D microscopy inside opaque objects with the CTAn® software program (Skyscan; Bruker). The vertical extent of the region of interest (ROI) was 4.0–5.0 mm. The boundary of the selected ROI was 8.0–8.5 mm in diameter. The grayscale histogram was set from 30 to 40 HU on the 1172 system and from 190 to 210 HU on the 1072 system to remove metal implant artifacts and to prevent the overestimation of

https://doi.org/10.5051/jpis.2300660033

regenerative values. The PCL-TCP scaffold was evaluated for reference value calibrations. The 3D analysis data of the reference PCL-TCP scaffold was 240.29 mm^2 in bone surface (BS) and 255.12 mm^3 in tissue volume (TV). To prevent overestimation of the values for metal artifact and PCL-TCP scaffold radiopacity, the reference HU levels of PCL-TCP scaffolds without implants were evaluated. These PCL-TCP scaffolds revealed radiopacity or regenerative bone values ranging from 0 to 15 HU, with none observed in the 30–40 HU range. To prevent implant fixture artifacts and obtain the least amount of metal blurring, the optimal HU range was selected using binary image threshold scales, which yielded a range of 30–40 HU.

The new bone formation capacity was analyzed using the morphometric parameters of total tissue volume (TV, mm^3), bone volume (BV, mm^3), regenerative new bone surface area (BS, mm^2), bone volume fraction ratio (BV/TV, %), bone surface density (BS/TV, mm^{-1}), bone specific surface (BS/BV, mm^{-1}), and interception surface (i.S, mm^2). Using the Vworks® software program (Osstem Implant Co.), 3D rendered models were obtained.

Histomorphometric analysis

The specimens were dehydrated and embedded in light curing resin (Technovit 7200 VLC+BPO; Kulzer & Co., Wehrheim, Germany). Then the blocks bearing implant scaffolds were cut along their long axis and reduced to a thickness of 30 μm using the Exakt Cutting and Grinding Equipment (Exakt Advanced Technologies GmbH, Norderstedt, Germany). Subsequently, these non-decalcified ground specimens were stained using hematoxylin-eosin and Masson's trichrome staining. Using the measuring and annotating modules of Kappa ImageBase® software (Kappa optronics GmbH, Gleichen, Germany), new bone height (NBH, mm), new bone area (NBA, mm^2), residual scaffold area (RSA, mm^2) and the bone-implant contact (BIC) ratio in the experimental sites exposed to the maxillary sinus were evaluated for histomorphometric analysis (**Figure 3**). NBH was defined as the maximal regenerative bone height from the interface between the maxillary sinus floor and the scaffold to the inner space of the scaffold or along the implant fixture surface.

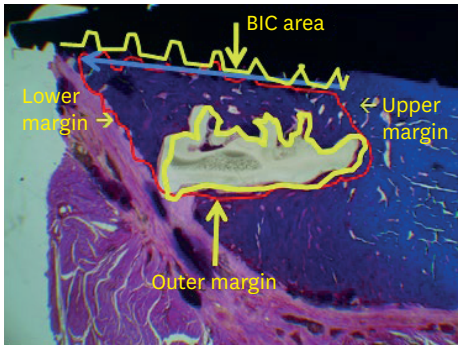

Figure 3. Parameters of the histomorphometric analysis. New bone height (blue arrow line, maximal regenerative bone height (mm) from the interface between the maxillary sinus floor and the scaffold to the inner space of the scaffold or along the implant fixture surface), new bone area (red polygonal area, the total regenerative bone area (mm^2) from the interface between the maxillary sinus floor and the scaffold to the inner or outer space of the scaffold or along the implant fixture surface), BIC in new bone height (red/yellow length ratio, the ratio of the total contact length between the implant fixture and the new bone within the new bone height area), and the residual scaffold area (yellow polygonal area, the total residual scaffold area (mm^2) in the experimental site following degradation) in the experimental area were calculated using Kappa image analyzer software.
BIC: bone-implant contact.

https://doi.org/10.5051/jpis.2300660033

Fluoromicroscopic evaluation

To evaluate the new bone formation sequence, the polychromic bone labeling samples were observed using a confocal laser-scanning microscope (Olympus-Flouview300; Olympus Co., Tokyo, Japan). Confocal images were obtained using filtering ranges of alizarin red (530–560/580 nm with red coding), calcein (494/517 nm with green coding), and Tc HCl (525–560 nm with yellow coding). Additionally, all images were taken under magnification using a ×10 objective lens and a 200 μm scale bar.

Statistics

One-way analysis of variance was utilized for multiple comparisons, followed by the Fisher protected least significant difference test for *post hoc* testing using Statview® statistical software (SAS Institute Inc., Cary, NC, USA). All data were reported as mean ± standard deviation. *P* values <0.05 were considered to indicate statistical significance.

RESULTS

Gross findings

The experiment was performed at 20 sites in 10 maxillary sinuses of 5 minipigs. The healing process was uneventful for each animal. Two implants in the PCL-TCP+hUCMSCs+PRP group and 2 implants in the PCL-TCP+PRP group were found to have floated into the sinuses, resulting in reduced specimen numbers in the PCL-TCP+hUCMSCs+PRP group (n=5) and the PCL-TCP+PRP group (n=5), compared to the PCL-TCP group (n=6).

Densitometric analysis

Significantly higher mean grayscale levels and ratios were found in the PCL-TCP+hUCMSCs+PRP group than in the PCL-TCP group ($P<0.05$). For the gray level and ratio of new bone formation (%), the PCL-TCP+hUCMSCs+PRP and PCL-TCP+PRP groups had higher mean values than the PCL-TCP group; however, there were no significant differences ($P=0.170$) (**Table 1**).

Three-dimensional bone morphogenic analysis

BS/BV was higher in the PCL-TCP+hUCMSCs+PRP group than in the PCL-TCP and PCL-TCP+PRP groups; however, these differences were not significant ($P=0.506$). The PCL-TCP+PRP group had higher mean values than the other groups for regenerative BV ($P=0.416$), BV/TV ($P=0.366$), and i.S ($P=0.269$), which is a useful measure in the evaluation of bone growth in a defined area. The PCL-TCP group had higher mean values than the other groups with respect to new BS and BS/TV. However, there were no significant differences among the parameters or the groups ($P=0.089$ and $P=0.179$, respectively) (**Table 2**).

Table 2. Bone morphogenic analysis by micro-computed tomography

Group	No.	BV (mm^3)	BV/TV (%)	BS (mm^2)	BS/TV (mm^{-1})	BS/BV (mm^{-1})	i.S (mm^2)
PCL-TCP+hUCMSCs+PRP	5	10.63±6.64	4.42±2.60	1,024.69±431.32	4.34±1.46	124.18±57.34	2.78±2.73
PCL-TCP+PRP	5	15.21±10.68	7.19±5.56	825.95±118.46	3.88±0.69	93.49±72.77	6.83±6.68
PCL-TCP	6	13.99±8.16	6.73±5.19	1,166.63±289.50	5.10±1.79	116.95±78.88	4.26±6.18

Values are presented as mean ± standard deviation.
For the reference PCL-TCP scaffold without the dental implant, TV was 255.12 mm^3 and BS was 240.29 mm^2.
BV: bone volume, BV/TV: bone volume fraction ratio, TV: total tissue volume, BS: regenerative new bone surface area, BS/TV: bone surface density, BS/BV: bone specific surface, i.S: interception surface, PCL-TCP: poly-(ε-caprolactone)/β-tricalcium phosphate, hUCMSC: human umbilical cord-derived mesenchymal stem cell, PRP: platelet-rich plasma.

https://doi.org/10.5051/jpis.2300660033

JPIS
Journal of Periodontal & Implant Science

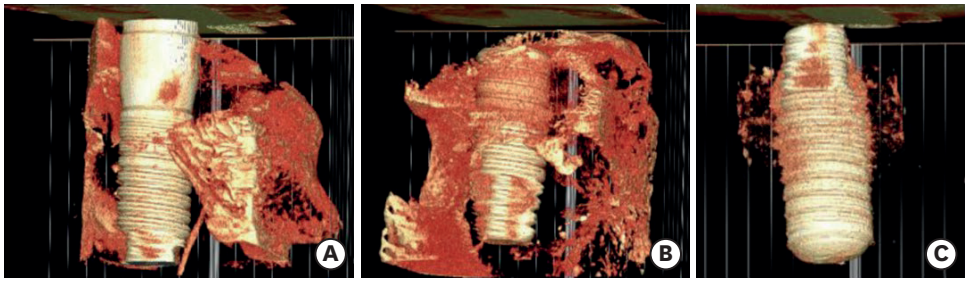

Figure 4. 3D rendered model of micro-CT at 12 weeks postoperatively. (A) PCL-TCP+hUCMSCs+PRP group, (B) PCL-TLP+PRP group, and (C) PCL-TCP group. Some regenerative bone formation along the implant fixture surfaces was observed in all groups, and more residual scaffold remnants were seen around the implant fixture in the PCL-TCP group than in the other groups.
PCL-TCP: poly-(ε-caprolactone)/β-tricalcium phosphate, hUCMSC: human umbilical cord-derived mesenchymal stem cell, PRP: platelet-rich plasma.

In the 3D reconstructed images, some degree of bone formation was observed along the surfaces of the implant fixtures in each group. More scaffolds were maintained around the implant fixture in the PCL-TCP group than in the other groups (**Figure 4**).

Histomorphometric analysis

In the histomorphometric analysis, each implant-grafted site in the slide images (×1.25 magnification) was calibrated with 4 parameters. The PCL-TCP+hUCMSCs+PRP group had significantly higher BIC values than the PCL-TCP group (P<0.05). As for NBH and NBA, the PCL-TCP+hUCMSCs+PRP group showed better results than the PCL-TCP and PCL-TCP+PRP groups; however, the values were not significantly different (P=0.056 and P=0.687, respectively) (**Table 3**). According to the results of the degradation rates (RSA), the PCL-TCP+hUCMSCs+PRP group had a greater rate of degradation than the other groups; however, this difference was not statistically significant (P=0.096) (**Table 3**).

Histological and fluoromicroscopic findings

In the PCL-TCP+hUCMSCs+PRP group, new bone formation and degradation of the scaffold without inflammatory reactions were seen from the interface between the sinus floor and the scaffold surface to the inner area of the scaffold. New bone formation around the outer surfaces of the scaffolds was observed, suggesting a tenting effect of the specially designed PCL-TCP scaffolds in the elevated sinus membranes; furthermore, bone regeneration occurred at the scaffold-implant interfaces (**Figure 5A-C**). In the fluoromicroscopic images, new bone formation was detected along part of the scaffold-implant interface. However, there were rare chronological ingrowth patterns of the new bone (**Figure 5D**).

In the PCL-TCP+PRP and PCL-TCP groups, new bone formation and scaffold degradation were also observed from the interfaces between the sinus floors and the scaffold surfaces

Table 3. Histomorphometric analysis

Group	No.	NBH (mm)	NBA (mm^2)	BIC	RSA (mm^2)
PCL-TCP+hUCMSCs+PRP	5	1.26±0.73	0.71±0.48	0.34±0.21[a)]	3.79±1.43
PCL-TCP+PRP	5	0.56±0.63	0.57±0.78	0.18±0.27	5.09±2.06
PCL-TCP	6	0.73±0.95	0.58±0.82	0.09±0.19[a)]	4.24±1.58

Values are presented as mean±standard deviation.
NBH: new bone height, NBA: new bone area, BIC: bone-implant contact, RSA: residual scaffold area, PCL-TCP: poly-(ε-caprolactone)/β-tricalcium phosphate, hUCMSC: human umbilical cord-derived mesenchymal stem cell, PRP: platelet-rich plasma.
[a)]A statistically significant difference between the PCL-TCP+hUCMSCs+PRP group and the PCL-TCP group was found, P<0.05, using analysis of variance with the *post hoc* Fisher protected least significant difference test.

https://doi.org/10.5051/jpis.2300660033

JPIS
Journal of Periodontal & Implant Science

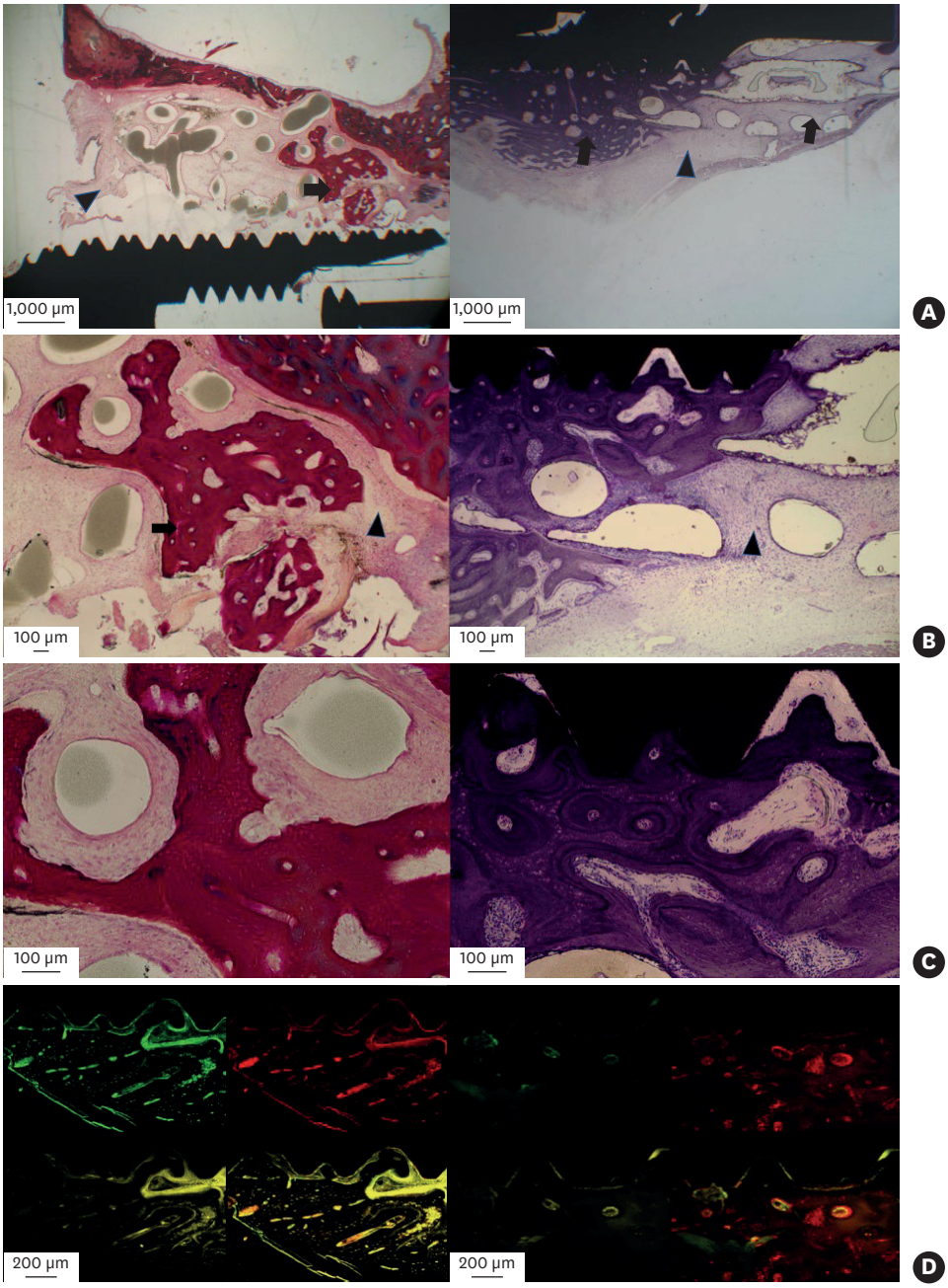

Figure 5. Histological and fluoromicroscopic images of the PCL-TCP+hUCMSCs+PRP group at 12 weeks postoperatively. (A) New bone formation and degradation of the scaffold without inflammatory reactions were observed from the interfaces between the sinus floor and the scaffold surface to the inner area of the scaffold. With the tenting effect of the scaffold in the elevated sinus membrane, new bone formation around the outer surface of the scaffold was seen (left side, hematoxylin-eosin staining). In addition, bone regeneration occurred at the BIC area (right side, Masson's trichrome staining). (B) New bone formation was observed amid the encapsulated residual degradable scaffold remnants (left side), and new bone ingrowths were seen in the implant thread area within the implant-scaffold interfaces (right side). (C) Uniform and dense stained woven bone-like structures were seen among micropores in the scaffold. (D) In laser scanning confocal images, chronological series from the lower left: vital staining with tetracycline HCl 3 weeks postoperatively (yellow), upper left: vital staining with calcein 6 weeks postoperatively (green), upper right: vital staining with alizarin red 9 weeks postoperatively (red), and lower right: vital staining with tetracycline HCl 11 weeks postoperatively. New bone formation activity was detected in the BIC area. However, there were rare chronological ingrowth patterns of new bone.
PCL-TCP: poly-(ε-caprolactone)/β-tricalcium phosphate, hUCMSC: human umbilical cord-derived mesenchymal stem cell, PRP: platelet-rich plasma, BIC: bone-implant contact.
Arrowhead: remaining scaffold, arrow: new bone.

https://doi.org/10.5051/jpis.2300660033

JPIS
Journal of Periodontal & Implant Science

to the scaffold-implant interface areas (**Figures 6A-6C** and **7A-7C**). The fluoromicroscopic findings of these two groups were largely similar to those of the PCL-TCP+hUCMSCs+PRP group (**Figures 6D** and **7D**).

DISCUSSION

The present study evaluated the efficacy of a PCL-TCP scaffold with hUCMSCs and PRP for bone regeneration during single-stage sinus augmentation and dental implantation in minipigs. This experiment revealed that the PCL-TCP scaffold with hUCMSCs and PRP presented the best NBH, NBA, and BIC values, and the use of these types of scaffolds could improve the osseointegration of dental implants placed in the porcine elevated sinus. However, there was no clear support for the effects of either the hUCMSCs or the PRP on bone regeneration, since clear differences were not observed between the PCL-TCP+hUCMSCs+PRP and PCL-TCP+PRP groups in *post hoc* testing. These results are consistent with previous studies, which reported that the transplantation of MSCs and PRP induces significant bone formation within osteoconductive carriers during sinus lifting or dental implantation [12,20,21]. In contrast to the hUCMSC- and PRP-supported methods, the scaffold with PCL-TCP alone failed to promote significant bone formation. These results

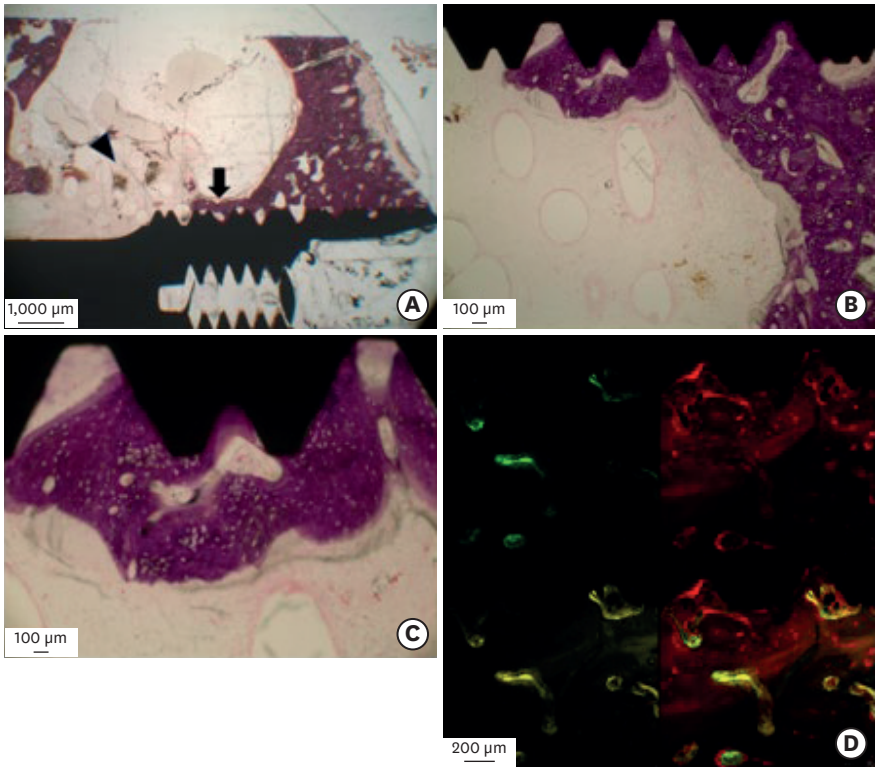

Figure 6. Histological and fluoromicroscopic images of the PCL-TCP+PRP group at 12 weeks postoperatively. (A) New bone formation (arrow) and degradation of the scaffold (arrowhead) without inflammatory reactions were observed from interfaces between the sinus floor and the scaffold surface to the BIC area. (B) New bone ingrowths were observed in the implant thread area within the implant-scaffold interfaces. (C) Mineralized structures with thin, stained, newly formed osteogenic tissues were seen in the implant-scaffold interface. (D) In laser-scanned confocal images, new bone formation activity was detected at the BIC area. However, there were rare chronological ingrowth patterns of new bone.
PCL-TCP: poly-ε-caprolactone β-tricalcium phosphate, PRP: platelet-rich plasma, BIC: bone-implant contact.

https://doi.org/10.5051/jpis.2300660033

JPIS
Journal of Periodontal & Implant Science

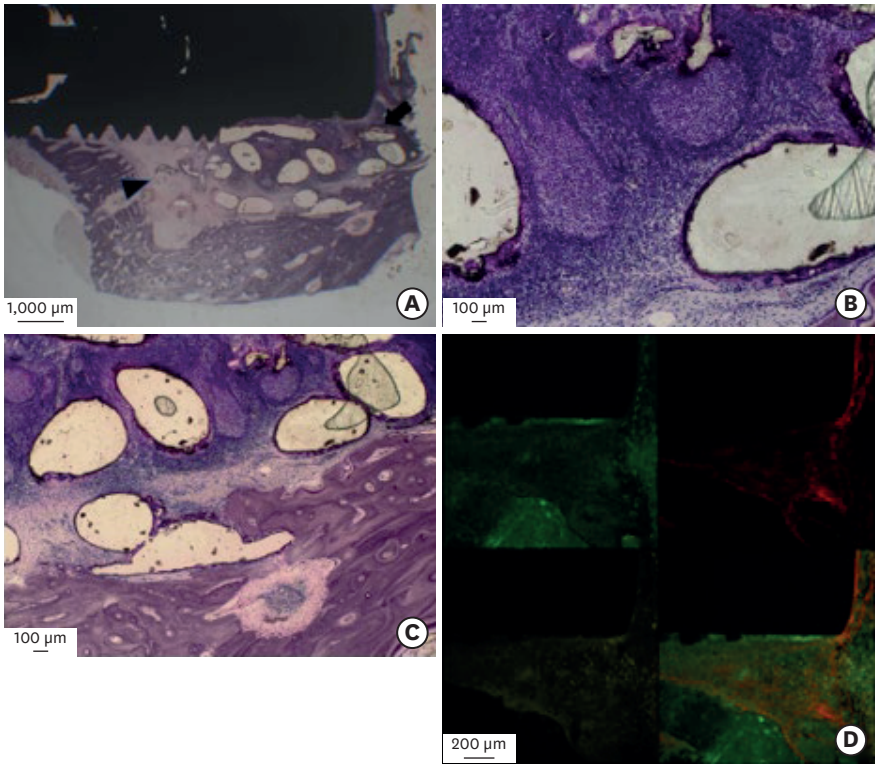

Figure 7. Histological and fluoromicroscopic images of the PCL-TCP group at 12 weeks postoperatively. (A) Immature bone formation was observed at the interfaces between the sinus floor and the scaffold surface (arrowhead). With the tenting effect of the scaffold in the elevated sinus membrane, new bone formation (arrow) around the outer surfaces of the scaffold was observed. However, the central region consisted of fibrosis and a few blood vessels with inflammatory changes. (B) and (C) A small amount of new bone ingrowth was seen in the lateral portion of the scaffold from the host bone and in the lifted sinus cavity area. However, inflammation occurred within the scaffold area. (D) In laser-scanned confocal images, a small amount of new bone formation activity was detected at the bone-implant contact area. However, there were rare chronological ingrowth patterns of the new bone.
PCL-TCP: poly-(ε-caprolactone) β-tricalcium phosphate, hUCMSC: human umbilical cord-derived mesenchymal stem cell, .

suggest that hUCMSCs may serve as a source of stem cells for bone regeneration, and that PCL-TCP scaffolds may be more effective when combined with hUCMSCs and PRP.

Though MSCs are known to have immune-suppressive effects, it was shown that porcine UCMSCs could be xenotransplanted into non-immune-suppressed rats, where they engrafted and proliferated in a controlled fashion, responded to local signals, and were differentiated along a neural lineage [22]. Following intrauterine transplantation of human MSCs into sheep, the cells persisted long-term and differentiated along multiple mesenchymal lineages [23]. Indirect support for an immune-suppressive effect of UCMSCs has also been reported by some research groups that transplanted UCMSCs xenogeneically in non-immune-suppressed hosts without immune rejection [22-25]. In placenta-derived MSCs, the results of endothelial (-), hematopoietic markers (-) and major histocompatibility complex I (low)/II (-) suggested that these lines had low immunogenicity and immune-suppressive effects following transplantation [26]. These data support the hypothesis that UCMSCs, like MSCs, may have immunosuppressive effects and may support hUCMSCs as applicable to porcine maxillary sinus augmentation.

https://doi.org/10.5051/jpis.2300660033

In this experiment, specially designed, tube-shaped PCL-TCP had the advantages of time saving during the sinus lifting and grafting procedures, with direct fitting into the implant fixtures and preservation of the elevated sinus membrane and the sinus cavity with a tenting effect. The function of the scaffold's inner structure was to improve primary implant stability, ensured through holding and friction fit effect, and the outer porous structure was used for loading the cells or growth factors. Additionally, there was no spreading-out tendency, which has been reported in conventional particulate bone-graft cases. In these experimental procedures, 4 of 20 specimens in the 5 minipigs failed through postoperative infection or floating loss, due to poor primary stability in the grafted materials and the dental implants. More complicated and time-consuming procedures with sinus lifting, stem-cell seeding, PRP loading into the scaffold, and dental implantation might result instead in increased levels of surgical complications. However, the PCL-TCP-only group suffered no failures. Therefore, it can be concluded that the current study's specially designed PCL-TCP scaffold had the advantages of encouraging implant-scaffold contact and preserving primary implant stability in deficient maxillary sinus-floor bones. Additionally, although the PCL-TCP-only group had lower bone regenerative values across most parameters, the tube-shaped PCL-TCP scaffold had some advantages with respect to easy and direct frictional fitting on the implant fixture, which results in faster surgical processing, time-saving, and better preservation of the lifted sinus. In this study, although non-threaded scaffolds were used due to technical difficulties in manufacturing, they had favorable levels of initial stability for implantation and an optimal structure for cell seeding and PRP loading. If a threaded structure on the inner surface of the PCL-TCP scaffold were manufactured for customized implant fixture threads with a bolt-nut design, then accelerated bone regeneration at the scaffold-implant interface area might occur, together with a greater increase in the implant's initial stability.

The internal pore architecture of the scaffold is an important factor in the process of tissue regeneration, since it directly affects cell penetration, nutrition diffusion, and bone matrix deposition [27]. A PCL-TCP scaffold with an interconnected pore structure [28,29] was used as the basic scaffold material in this study. It has been reported that composite scaffolds of PCL with 20% 100-300 μm micro-particle β-TCP have biodegradable and bioactive properties [30,31]. These PCL-TCP scaffolds are permeable to cellular and vascular infiltration when implanted [32]. The 3D scaffolds provided the support necessary for cellular activity, including adherence, proliferation, and differentiation [29-31]. Scaffolds made of polycaprolactone were reported to have load-bearing capacities in bone tissue engineering applications [33]. These scaffolds had a slower degradation rate with structural degradation kinetics of only 7% of their volume over a 6-month period *in vivo*, and they maintained mechanical support for a sustained period of time [34]. Additionally, the slow rate of degradation reduced the risk of acidosis by preventing the rapid accumulation of acidic by-products, suggesting its use for bone tissue engineering.

In this experiment, PRP was selected as a contributing factor, based on evidence that growth factors such as PDGF, TGF-β, and IGF-I are released by the platelet gel and enhance reparative processes including osteogenesis and angiogenesis. It was postulated that the transplantation of several angiogenic inducers with MSCs combined with PRP promoted greater initial angiogenesis and better penetration of the cells into the core of the scaffold, resulting in rapid and sustained osteogenesis [35,36]. MSCs may provide an osteogenic cell source for new bone formation, and PRP may improve proliferation of MSCs, retaining their differentiation and in vivo bone formation capacities. Therefore, the positive effects of MSCs and PRP on osseointegration in the present study suggest that the required concentrations of

https://doi.org/10.5051/jpis.2300660033

osteogenic cells and growth factors in the hUCMSCs and the PRP conditions may have been achieved. However, to fully examine the individual contributions of the hUCMSCs and the PRP to bone regeneration, further study will be required.

In this study, the PCL-TCP+hUCMSCs+PRP group's parameters did not always indicate favorable values of bone regeneration. There may be some considerations when using these types of scaffolds, including obtaining a sufficient amount of stem cell seeding, establishing a homogeneous cell distribution, obtaining an appropriate level of immunoreactivity in the hUCMSCs of the porcine host, and maintaining stem cell viability following the operation. Some methods for homogenous cellular seeding and extracellular matrix distribution include using bioreactors with a uniaxial or biaxial design and treating the chemical surface of the PCL scaffold with 5 M sodium hydroxide for 12 hours to improve surface roughness and hydrophilicity before cells are seeded [37]. Bioreactors improve the efficiency of mass transfer by accelerating the perfusion of cellular scaffolds. Additionally, they trigger the mechano-transduction signaling pathway by providing mechanical stimulation, which leads to osteogenic differentiation among MSC cell types [14]. Although our study did not use a bioreactor, the use of bioreactors in studies of cell dispersal into scaffolds would be beneficial.

This study has limitations. There were no negative control groups with which to compare the efficacy of the specially designed scaffold. Furthermore, 4 implant attempts failed, even though some complex treatments were added in the PCL-TCP+hUCMSCs+PRP and PCL-TCP+PRP groups. The failure rate was somewhat higher compared to the clinical results. However, similar results were reported by Pieri et al. [12], wherein 1 of the 8 minipigs experienced wound infections in both sinuses, one with hydroxyapatite and the other with hydroxyapatite, MSC, and PRP. It seemed that the complex procedures increased minor inflammation and led to implant failure, although the procedures were done under sterile conditions. Despite the limitations of this study, fluoromicroscopic images of new bone formation around the outer surfaces of the scaffolds in the PCL-TCP+hUCMSCs+PRP group demonstrated the potential of the scaffold used in this study, and further investigation is necessary.

In conclusion, a specially designed, tube-shaped PCL-TCP (20%) composite scaffold with hUCMSCs and PRP enhanced bone formation in single-stage sinus augmentation and dental implantation in minipigs, compared to the use of a PCL-TCP scaffold alone. This honeycombed scaffold design may be mechanically advantageous for tissue-engineered bone regeneration.

REFERENCES

1. Jensen OT, Shulman LB, Block MS, Iacono VJ. Report of the Sinus Consensus Conference of 1996. Int J Oral Maxillofac Implants 1998;13 Suppl:11-45.
PUBMED
2. Wood RM, Moore DL. Grafting of the maxillary sinus with intraorally harvested autogenous bone prior to implant placement. Int J Oral Maxillofac Implants 1988;3:209-14.
PUBMED
3. Nkenke E, Weisbach V, Winckler E, Kessler P, Schultze-Mosgau S, Wiltfang J, et al. Morbidity of harvesting of bone grafts from the iliac crest for preprosthetic augmentation procedures: a prospective study. Int J Oral Maxillofac Surg 2004;33:157-63.
PUBMED | CROSSREF
4. Nasr HF, Aichelmann-Reidy ME, Yukna RA. Bone and bone substitutes. Periodontol 2000 1999;19:74-86.
PUBMED | CROSSREF

https://doi.org/10.5051/jpis.2300660033

5. Ozbek B, Erdogan B, Ekren N, Oktar FN, Akyol S, Ben-Nissan B, et al. Production of the novel fibrous structure of poly(ε-caprolactone)/tri-calcium phosphate/hexagonal boron nitride composites for bone tissue engineering. J Aust Ceram Soc 2018;54:251-60.
CROSSREF
6. Huang B, Caetano G, Vyas C, Blaker JJ, Diver C, Bártolo P. Polymer-ceramic composite scaffolds: the effect of hydroxyapatite and β-tri-calcium phosphate. Materials (Basel) 2018;11:129.
PUBMED | CROSSREF
7. Lee JW, Chu SG, Kim HT, Choi KY, Oh EJ, Shim JH, et al. Osteogenesis of adipose-derived and bone marrow stem cells with polycaprolactone/tricalcium phosphate and three-dimensional printing technology in a dog model of maxillary bone defects. Polymers (Basel) 2017;9:450.
PUBMED | CROSSREF
8. Shim JH, Won JY, Park JH, Bae JH, Ahn G, Kim CH, et al. Effects of 3D-printed polycaprolactone/β-tricalcium phosphate membranes on guided bone regeneration. Int J Mol Sci 2017;18:899.
PUBMED | CROSSREF
9. Hutmacher DW. Scaffolds in tissue engineering bone and cartilage. Biomaterials 2000;21:2529-43.
PUBMED | CROSSREF
10. Wang Y, Uemura T, Dong J, Kojima H, Tanaka J, Tateishi T. Application of perfusion culture system improves *in vitro* and *in vivo* osteogenesis of bone marrow-derived osteoblastic cells in porous ceramic materials. Tissue Eng 2003;9:1205-14.
PUBMED | CROSSREF
11. Kang SH, Park JB, Kim I, Lee W, Kim H. Assessment of stem cell viability in the initial healing period in rabbits with a cranial bone defect according to the type and form of scaffold. J Periodontal Implant Sci 2019;49:258-67.
PUBMED | CROSSREF
12. Pieri F, Lucarelli E, Corinaldesi G, Iezzi G, Piattelli A, Giardino R, et al. Mesenchymal stem cells and platelet-rich plasma enhance bone formation in sinus grafting: a histomorphometric study in minipigs. J Clin Periodontol 2008;35:539-46.
PUBMED | CROSSREF
13. Safi IN, Hussein BM, Al-Shammari AM. Bio-hybrid dental implants prepared using stem cells with β-TCP-coated titanium and zirconia. J Periodontal Implant Sci 2022;52:242-57.
PUBMED | CROSSREF
14. Bilodeau K, Mantovani D. Bioreactors for tissue engineering: focus on mechanical constraints. A comparative review. Tissue Eng 2006;12:2367-83.
PUBMED | CROSSREF
15. Song K, Liu T, Cui Z, Li X, Ma X. Three-dimensional fabrication of engineered bone with human bio-derived bone scaffolds in a rotating wall vessel bioreactor. J Biomed Mater Res A 2008;86:323-32.
PUBMED | CROSSREF
16. Sikavitsas VI, Bancroft GN, Mikos AG. Formation of three-dimensional cell/polymer constructs for bone tissue engineering in a spinner flask and a rotating wall vessel bioreactor. J Biomed Mater Res 2002;62:136-48.
PUBMED | CROSSREF
17. Zhang ZY, Teoh SH, Chong WS, Foo TT, Chng YC, Choolani M, et al. A biaxial rotating bioreactor for the culture of fetal mesenchymal stem cells for bone tissue engineering. Biomaterials 2009;30:2694-704.
PUBMED | CROSSREF
18. Almansoori AA, Kwon OJ, Nam JH, Seo YK, Song HR, Lee JH. Mesenchymal stem cells and platelet-rich plasma-impregnated polycaprolactone-β tricalcium phosphate bio-scaffold enhanced bone regeneration around dental implants. Int J Implant Dent 2021;7:35.
PUBMED | CROSSREF
19. Lee J, Susin C, Rodriguez NA, de Stefano J, Prasad HS, Buxton AN, et al. Sinus augmentation using rhBMP-2/ACS in a mini-pig model: relative efficacy of autogenous fresh particulate iliac bone grafts. Clin Oral Implants Res 2013;24:497-504.
PUBMED | CROSSREF
20. Ohya M, Yamada Y, Ozawa R, Ito K, Takahashi M, Ueda M. Sinus floor elevation applied tissue-engineered bone. Comparative study between mesenchymal stem cells/platelet-rich plasma (PRP) and autogenous bone with PRP complexes in rabbits. Clin Oral Implants Res 2005;16:622-9.
PUBMED | CROSSREF
21. Ito K, Yamada Y, Naiki T, Ueda M. Simultaneous implant placement and bone regeneration around dental implants using tissue-engineered bone with fibrin glue, mesenchymal stem cells and platelet-rich plasma. Clin Oral Implants Res 2006;17:579-86.
PUBMED | CROSSREF

22. Weiss ML, Mitchell KE, Hix JE, Medicetty S, El-Zarkouny SZ, Grieger D, et al. Transplantation of porcine umbilical cord matrix cells into the rat brain. Exp Neurol 2003;182:288-99.
PUBMED | CROSSREF

23. Weiss ML, Troyer DL. Stem cells in the umbilical cord. Stem Cell Rev 2006;2:155-62.
PUBMED | CROSSREF

24. Medicetty S, Bledsoe AR, Fahrenholtz CB, Troyer D, Weiss ML. Transplantation of pig stem cells into rat brain: proliferation during the first 8 weeks. Exp Neurol 2004;190:32-41.
PUBMED | CROSSREF

25. Fu YS, Cheng YC, Lin MY, Cheng H, Chu PM, Chou SC, et al. Conversion of human umbilical cord mesenchymal stem cells in Wharton's jelly to dopaminergic neurons in vitro: potential therapeutic application for Parkinsonism. Stem Cells 2006;24:115-24.
PUBMED | CROSSREF

26. Portmann-Lanz CB, Schoeberlein A, Huber A, Sager R, Malek A, Holzgreve W, et al. Placental mesenchymal stem cells as potential autologous graft for pre- and perinatal neuroregeneration. Am J Obstet Gynecol 2006;194:664-73.
PUBMED | CROSSREF

27. Hollister SJ, Levy RA, Chu TM, Halloran JW, Feinberg SE. An image-based approach for designing and manufacturing craniofacial scaffolds. Int J Oral Maxillofac Surg 2000;29:67-71.
PUBMED | CROSSREF

28. Hutmacher DW, Schantz T, Zein I, Ng KW, Teoh SH, Tan KC. Mechanical properties and cell cultural response of polycaprolactone scaffolds designed and fabricated via fused deposition modeling. J Biomed Mater Res 2001;55:203-16.
PUBMED | CROSSREF

29. Zein I, Hutmacher DW, Tan KC, Teoh SH. Fused deposition modeling of novel scaffold architectures for tissue engineering applications. Biomaterials 2002;23:1169-85.
PUBMED | CROSSREF

30. Rai B, Teoh SH, Ho KH, Hutmacher DW, Cao T, Chen F, et al. The effect of rhBMP-2 on canine osteoblasts seeded onto 3D bioactive polycaprolactone scaffolds. Biomaterials 2004;25:5499-506.
PUBMED | CROSSREF

31. Rai B, Teoh SH, Hutmacher DW, Cao T, Ho KH. Novel PCL-based honeycomb scaffolds as drug delivery systems for rhBMP-2. Biomaterials 2005;26:3739-48.
PUBMED | CROSSREF

32. Feinberg SE, Aghaloo TL, Cunningham LL Jr. Role of tissue engineering in oral and maxillofacial reconstruction: findings of the 2005 AAOMS Research Summit. J Oral Maxillofac Surg 2005;63:1418-25.
PUBMED | CROSSREF

33. Sung HJ, Meredith C, Johnson C, Galis ZS. The effect of scaffold degradation rate on three-dimensional cell growth and angiogenesis. Biomaterials 2004;25:5735-42.
PUBMED | CROSSREF

34. Lam CX, Hutmacher DW, Schantz JT, Woodruff MA, Teoh SH. Evaluation of polycaprolactone scaffold degradation for 6 months *in vitro* and *in vivo*. J Biomed Mater Res A 2009;90:906-19.
PUBMED | CROSSREF

35. Roldán JC, Jepsen S, Schmidt C, Knüppel H, Rueger DC, Açil Y, et al. Sinus floor augmentation with simultaneous placement of dental implants in the presence of platelet-rich plasma or recombinant human bone morphogenetic protein-7. Clin Oral Implants Res 2004;15:716-23.
PUBMED | CROSSREF

36. Vogel JP, Szalay K, Geiger F, Kramer M, Richter W, Kasten P. Platelet-rich plasma improves expansion of human mesenchymal stem cells and retains differentiation capacity and *in vivo* bone formation in calcium phosphate ceramics. Platelets 2006;17:462-9.
PUBMED | CROSSREF

37. Schantz JT, Teoh SH, Lim TC, Endres M, Lam CX, Hutmacher DW. Repair of calvarial defects with customized tissue-engineered bone grafts I. Evaluation of osteogenesis in a three-dimensional culture system. Tissue Eng 2003;9 Suppl 1:S113-26.
PUBMED | CROSSREF

https://doi.org/10.5051/jpis.2300660033